RSC Advances

PAPER

View Article Online
View Journal | View Issue

Cite this: *RSC Adv.*, 2023, **13**, 21296

Benzoate-based thermally activated delayed fluorescence materials†

Liang Zhang, *[a] Wenjing Zhu,[a] Kangkang Gao,[a] Yun Wu,[a] Yani Lu,[a] Chao Shuai,[a] Penghui Zhang,[a] Huicheng Li[a] and Chuan-Feng Chen *[bc]

Received 17th May 2023
Accepted 10th July 2023

DOI: 10.1039/d3ra03289b

rsc.li/rsc-advances

Compounds **PTZ-MBZ** (methyl 3-(10*H*-phenothiazin-10-yl)benzoate) and **DMAC-MBZ** (methyl 3-(9,9-dimethylacridin-10(9*H*)-yl)benzoate) were conveniently synthesized, and they exhibited TADF properties with lifetimes of 0.80 and 2.17 μs, respectively. The spatially separated highest occupied molecular orbital and lowest unoccupied molecular orbital resulted in a very small singlet–triplet energy gap of 0.0152 eV and 0.0640 eV, respectively. Thermally activated delayed fluorescence materials with short lifetime could be used as promising luminescent materials for organic light-emitting diodes.

Thermally activated delayed fluorescence (TADF) materials[1–3] have aroused increasing interest, and thus have also become the third-generation organic luminescent materials[4–6] after fluorescent and phosphorescent materials.[7] As the third-generation organic luminescent materials, TADF materials display a special radiative transition *via* reverse intersystem crossing (RISC) of excitons from the lowest triplet (T_1)[8–10] to the lowest singlet (S_1) state,[11] and thus obtain a high theoretical quantum yield of 100%.[12–14] Generally, TADF molecules are designed by introducing a twisted angle between acceptor and donor moieties[15,16] to avoid the overlap between lowest unoccupied molecular orbital (LUMO) and the highest occupied molecular orbital (HOMO).[17–20]

In general, the lifetime of a TADF material is in a range of hundreds of microseconds as a result of its endothermic RISC process.[21–25] Most TADF materials reveal long delayed fluorescent lifetime,[26–29] which lead to enhance the triplet-related nonradiative process,[30–34] such as triplet–triplet annihilate (TTA), triplet-polaron annihilate (TPA), and severely efficiency roll-off at high current density. So far, various electron-accepting moieties have been applied as receptors for the design and construction of TADF molecules. However, benzoate group has rarely been used as receptor to study their TADF property.

Herein, we report two novel TADF emitters **PTZ-MBZ** (methyl 3-(10*H*-phenothiazin-10-yl)benzoate) and **DMAC-MBZ** (methyl 3-(9,9-dimethylacridin-10(9*H*)-yl)benzoate) with benzoate as electron acceptor (Fig. 1), which not only showed TADF property in films, but also exhibited short lifetime. Especially, thermally activated delayed fluorescence materials with short lifetime would be used as the promising luminescent materials for the organic light-emitting diode.

Compound **DMAC-MBZ** was conveniently synthesized by palladium catalyzed cross-coupling reactions of methyl 3-bromobenzoate with 9,9-dimethyl-9,10-dihydroacridine. Compound **PTZ-MBZ** was synthesized using similar synthetic steps. The compounds **PTZ-MBZ** and **DMAC-MBZ** could be easily synthesized in good yields. Their structures were confirmed by 1H NMR, 13C NMR, HRMS spectra.

The UV-vis absorption spectra of **PTZ-MBZ** and **DMAC-MBZ** in tetrahydrofuran were shown in Fig. 2a. Owing to their similar structures, the absorption bands of the two compounds are similar. These compounds showed a broad absorption band 258, 284 and 316 nm, which were assigned to π–π* transitions. Their absorption band range 395 nm and 396 nm can be assigned to the strong intermolecular charge transfer (ICT) between the phenothiazine donor moieties to benzoate acceptor group. As shown in Fig. 2b, we can achieve color

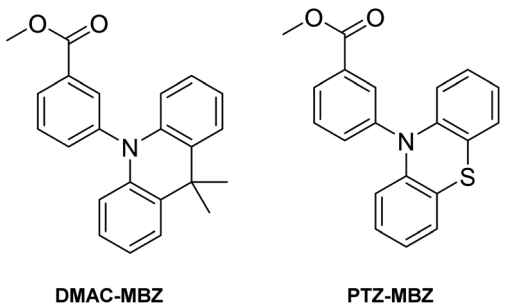

DMAC-MBZ PTZ-MBZ

Fig. 1 Structures of DMAC-MBZ and PTZ-MBZ.

[a]*College of Petrochemical Engineering, Longdong University, Qingyang 745000, China. E-mail: zhang_liang1113@126.com*

[b]*Beijing National Laboratory for Molecular Sciences, CAS Key Laboratory of Molecular Recognition and Function, Institute of Chemistry, Chinese Academy of Sciences, Beijing 100190, China. E-mail: cchen@iccas.ac.cn*

[c]*University of Chinese Academy of Sciences, Beijing 100049, China*

† Electronic supplementary information (ESI) available: Synthesis and characterization data of new compounds. See DOI: https://doi.org/10.1039/d3ra03289b

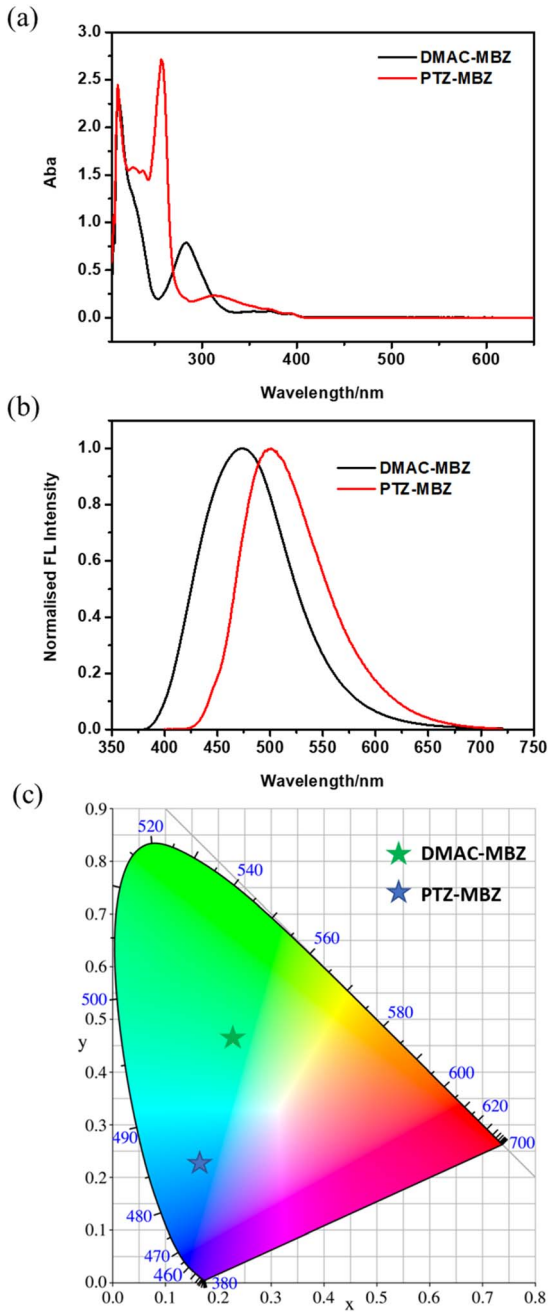

Fig. 2 (a) Absorption spectra of PTZ-MBZ and DMAC-MBZ in THF at room temperature; (b) fluorescence spectra of PTZ-MBZ and DMAC-MBZ in neat films at room temperature. (c) The CIE coordinates of the PL (CIE 1931 chromaticity coordinate calculation).

regulation by regulating the strength of ICT transition. The maximum fluorescence emission peaks are red-shifted on increase of the donor's electron donating ability, and are 501 and 474 nm for **PTZ-MBZ** and **DMAC-MBZ**, respectively. Absolute PLQYs of **PTZ-MBZ** and **DMAC-MBZ** in films were 74.02 and 55.12%, respectively. The chromatic coordinates of these luminescent compounds have also been studied (Fig. 2c). For **PTZ-MBZ** and **DMAC-MBZ**, their fluorescence CIE coordinates were found to be at (0.1666, 0.2238) and (0.2299, 0.4591), respectively.

The transient PL spectra of **PTZ-MBZ** and **DMAC-MBZ** in films were further conducted to determine whether the triplet excited states were involved in the delayed luminescence. As shown in Fig. 3a, it was found that the DF lifetimes of **PTZ-MBZ** and **DMAC-MBZ** in neat films at room temperature were 0.80 and 2.17 μs, respectively. It was found that these compounds displayed a distinctive microsecond-scaled delayed relaxation at room temperature, which implied the TADF properties of the emitters. Moreover, the temperature-dependent transient PL of **PTZ-MBZ** and **DMAC-MBZ** (Fig. 3b and c) was then investigated. The ratio of the delayed component gradually increased from 100 K to 300 K, demonstrating the typical characteristics of TADF for these emitters.

The density functional theory (DFT) calculation for all molecules were performed using GAUSSIAN 09W package.[35] All the molecules were optimized following the functional of with

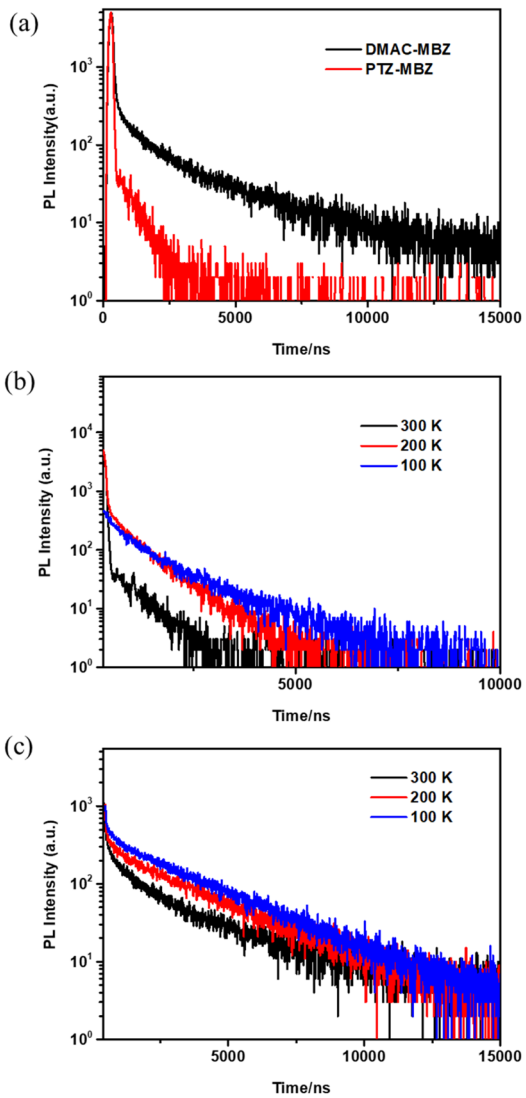

Fig. 3 (a) Transient decay spectra of PTZ-MBZ and DMAC-MBZ in a neat film at room temperature. The temperature-dependent transient photoluminescence spectra of (b) PTZ-MBZ and (c) DMAC-MBZ in the neat films.

Becke-3-Yang-Parr (B3LYP) combined with the basis set of def2-SVP (Ahlrich split-valence basis set with polarization functions on heavy atoms). Note that, the dispersion corrections for the non-bonding vdW interaction were carried out through the Grimme approach using atom pair-wise additive schemes, so-called DFT-D3 method. Finally, the excited states of all optimized structures were further investigated at the accuracy level of wB97XD/TZVP. The optimized geometry and the electron density distribution of **PTZ-MBZ** and **DMAC-MBZ** were investigated by density functional theory calculations (Fig. 4). Five compounds all showed the separated HOMO and LUMO distributions on their optimized geometries. The HOMOs are predominantly located on the electron-donating subunit, whereas the LUMOs are distributed over the electron-withdrawing benzoate group. The frontier molecular orbital of **PTZ-MBZ** and **DMAC-MBZ** showed small overlap mainly on the donor and acceptor units, resulting in the appreciable ΔE_{ST} values, evidenced by the calculated ΔE_{ST} values of 0.0152 eV and 0.0640 eV, respectively. Small ΔE_{ST} values led to high efficiency of the RISC, which could induce the TADF capability.

In conclusion, we have conveniently synthesized compound **PTZ-MBZ** and **DMAC-MBZ**, and found that it exhibited TADF properties with the lifetime of 0.80 and 2.17 μs, respectively. By connecting donor group with benzoate unit, realizing effective separation between HOMO and LUMO. The negligible overlap between HOMO and LUMO enables its CT character and a small ΔE_{ST}. The small ΔE_{ST} facilitate the fast RISC process and reduce the delayed fluorescence lifetime. Thermally activated delayed fluorescence materials with short lifetime would be used as the promising luminescent materials for the organic light emitting diode.

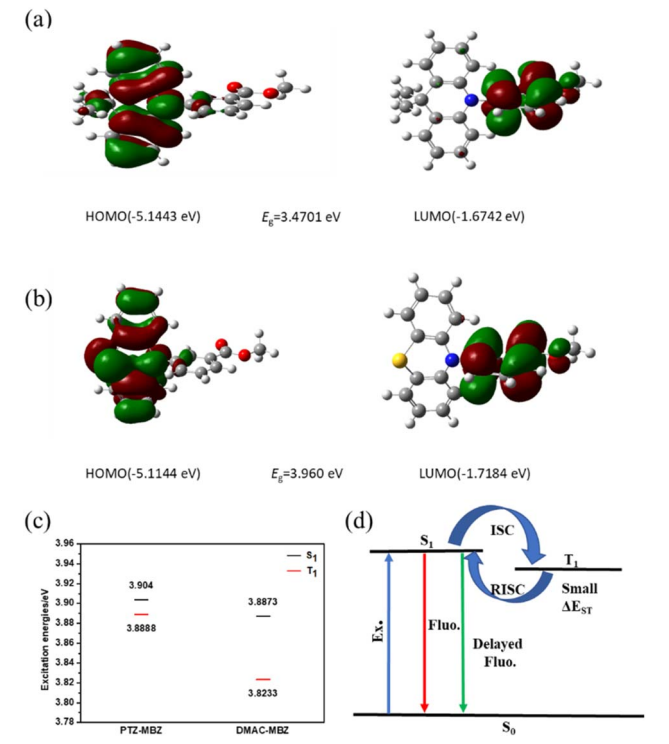

Fig. 4 Calculated spatial distributions of the HOMO and LUMO energy densities of (a) DMAC-MBZ and (b) PTZ-MBZ. (c) Excited state energy diagram. (d) Schematic energy levels diagram.

Conflicts of interest

There are no conflicts to declare.

Acknowledgements

This work was supported by the Doctoral Start-up Founds from Longdong University (No. XYBY202015), the Youth Science Foundation of Gansu Province (No. 21JR7RM194), the Youth Science and Technology Foundation of Qingyang City (No. QY-STK-2022A-007) and Higher Education Innovation Ability Improvement project of Gansu Province (No. 2022A-131).

Notes and references

1 H. Uoyama, K. Goushi, K. Shizu, H. Nomura and C. Adachi, *Nature*, 2012, **492**, 234–238.
2 X. Y. Cai and S. J. Su, *Adv. Funct. Mater.*, 2018, **28**, 1802558.
3 Y. Liu, X. Wu, Y. Chen, L. Chen, H. Li, S. Wang, H. Tian, H. Tong and L. Wang, *J. Mater. Chem. C*, 2019, **7**, 9719–9725.
4 Q. Wang, Q. S. Tian, Y. L. Zhang, X. Tang and L. S. Liao, *J. Mater. Chem. C*, 2019, **7**, 11329–11360.
5 X. Liang, Z.-L. Tu and Y.-X. Zheng, *Chem.–Eur. J.*, 2019, **25**, 5623–5642.
6 J. Xu, X. Zhu, J. Guo, J. Fan, J. Zeng, S. Chen, Z. Zhao and B. Z. Tang, *ACS Mater. Lett.*, 2019, **1**, 613–619.
7 Y. Tao, R. Chen, H. Li, J. Yuan, Y. Wan, H. Jiang, C. Chen, Y. Si, C. Zheng, B. Yang, G. Xing and W. Huang, *Adv. Mater.*, 2018, **30**, 1803856.
8 T. Huang, X. Song, M. Cai, D. Zhang and L. Duan, *Mater. Today Energy*, 2021, **21**, 100705.
9 H. Xu, Z. Li, D. Yang, C. Han, B. Zhao, H. Wang, P. Ma, P. Chang and D. Ma, *Angew. Chem., Int. Ed.*, 2021, **60**, 14846–14851.
10 M. Ma, J. Li, D. Liu, Y. Mei and R. Dong, *ACS Appl. Mater. Interfaces*, 2021, **13**, 44615–44627.
11 D. Liu, M. Zhang, H. Chen, D. Ma, W. Tian, K. Sun, W. Jiang and Y. Sun, *J. Mater. Chem. C*, 2021, **9**, 1221–1227.
12 L. Poulard, S. Kasemthaveechok, M. Coehlo, R. A. Kumar, L. Frédéric, P. Sumsalee, T. d'Anfray, S. Wu, J. Wang, T. Matulaitis, J. Crassous, E. Zysman-Colman, L. Favereau and G. Pieters, *Chem. Commun.*, 2022, **58**, 6554–6557.
13 Z. G. Wu, H. B. Han, Z. P. Yan, X. F. Luo, Y. Wang, Y. X. Zheng, J. L. Zuo and Y. Pan, *Adv. Mater.*, 2019, **31**, 1900524.
14 H. Liu, H. Liu, J. Fan, J. Guo, J. Zeng, F. Qiu, Z. Zhao and B. Z. Tang, *Adv. Opt. Mater.*, 2020, **8**, 2001027.
15 Z. Qiu, W. Xie, Z. Yang, J. H. Tan, Z. Yuan, L. Xing, S. Ji, W. C. Chen, Y. Huo and S. J. Su, *Chem. Eng. J.*, 2021, **415**, 128949.
16 Z. Huang, Z. Bin, R. Su, F. Yang, J. Lan and J. You, *Angew. Chem., Int. Ed.*, 2020, **59**, 9992–9996.

17 Z. Lv, J. Hou, J. Yao, Y. Yuan, Y. Qian, J. Zhu, H. Zhao, X. Xiong and C. Jiao, *RSC Adv.*, 2022, **12**, 11477–11483.
18 L. Yu, Z. Wu, G. Xie, W. Zeng, D. Ma and C. Yang, *Chem. Sci.*, 2018, **9**, 1385–1391.
19 Y. Liu, Y. Chen, H. Li, S. Wang, X. Wu, H. Tong and L. Wang, *ACS Appl. Mater. Interfaces*, 2020, **12**, 30652–30658.
20 Q. Li, J. Hu, J. Lv, X. Wang, S. Shao, L. Wang, X. Jing and F. Wang, *Angew. Chem., Int. Ed.*, 2020, **59**, 20174–20182.
21 G. Xia, C. Qu, Y. Zhu, J. Ye, K. Ye, Z. Zhang and Y. Wang, *Angew. Chem., Int. Ed.*, 2021, **60**, 9598–9603.
22 L. Zhang, Y. F. Wang, M. Li, Q. Y. Gao and C.-F. Chen, *Chin. Chem. Lett.*, 2020, **32**, 740–744.
23 H. J. Kim, H. Kang, J. E. Jeong, S. H. Park, C. W. Koh, C. W. Kim, H. Y. Woo, M. J. Cho, S. Park and D. H. Choi, *Adv. Funct. Mater.*, 2021, **31**, 2102588.
24 K. Matsuo and T. Yasuda, *Chem. Sci.*, 2019, **10**, 10687–10697.
25 Y. Wang, Y. Zhu, X. Lin, Y. Yang, B. Zhang, H. Zhan, Z. Xie and Y. Cheng, *J. Mater. Chem. C*, 2018, **6**, 568–574.
26 A. Nyga, T. Kaihara, T. Hosono, M. Sipala, P. Stachelek, N. Tohnai, S. Minakata, L. E. d. Sousa, P. d. Silva, P. Data and Y. Takeda, *Chem. Commun.*, 2022, **58**, 5889–5892.
27 Z. Lv, J. Hou, J. Yao, Y. Yuan, Y. Qian, J. Zhu, H. Zhao, X. Xiong and C. Jiao, *RSC Adv.*, 2022, **12**, 11477–11483.
28 H. Gao, Z. Li, Z. Pang, Y. Qin, G. Liu, T. Gao, X. Dong, S. Shen, X. Xie, P. Wang, C.-S. Lee and Y. Wang, *ACS Appl. Mater. Interfaces*, 2023, **15**, 5529–5537.
29 H. Xu, B. Zhao, H. Wang, C. Han, P. Ma, Z. Li and P. Chang, *Angew. Chem., Int. Ed.*, 2020, **59**, 19042–19047.
30 D. G. Congrave, B. H. Drummond, P. J. Conaghan, H. Francis, S. T. E. Jones, C. P. Grey, N. C. Greenham, D. Credgington and H. Bronstein, *J. Am. Chem. Soc.*, 2019, **141**, 18390–18394.
31 M. Monka, I. E. Serdiuk, K. Kozakiewicz, E. Hoffman, J. Szumilas, A. Kubicki, S. Y. Park and P. Bojarski, *J. Mater. Chem. C*, 2022, **10**, 7925–7934.
32 C. Leng, S. You, Y. Si, H.-M. Qin, J. Liu, W.-Q. Huang and K. Li, *J. Phys. Chem. A*, 2021, **125**, 2905–2912.
33 B. Huang and O. A. von Lilienfeld, *Nat. Chem.*, 2020, **12**, 945–951.
34 L. Huang, Y. Sun, G. Zhao, L. Wang, X. Meng, J. Zhou and H. Duan, *J. Mol. Struct.*, 2022, **1255**, 132427.
35 Y. Wang, W. Wu and K. L. Choy, *J. Phys. Org. Chem.*, 2022, **35**, e4386.